Electrodynamic interaction between a nanoparticle and the surface of a solid

Dmytro Kysylychyn, Volodymyr Piatnytsia, and Valeri Lozovski*

Institute of High Technologies, Taras Shevchenko National University of Kyiv, 64 Volodymyrska street, Kyiv, 01601, Ukraine

We study the interaction between a nanoparticle and the surface of a solid in the framework of the local-field method. Assuming that the nanoparticle is characterized by a finite nonlinear polarizability, we obtain the interaction potential that is repulsive at short range and has an attractive long-range tail. Our numerical analysis shows that this potential strongly depends on the shape and size of the particle. Further, we study the particle-surface interaction in the presence of a surface plasmon polariton propagating along the interface. It is shown that the excitation of the surface wave leads to a drastic (about one order of magnitude) increase in the binding energy. Potential applications of this effect are discussed.

I. INTRODUCTION

Rapid development of nanotechnologies has led to an increased interest among researchers in the fundamental properties of the interaction between nanoparticles (or molecules) and the surface of a solid. This interaction determines the adsorption properties [1,2], lies at the origin of such effects as surface-enhanced Raman spectroscopy (SERS) [3,4] and local-field-enhanced luminescence [5–7], and constitutes the base of several modern nanomanufacturing techniques [8–10]. A number of methods of visualizing nanoparticles on the surface, such as various scanning microscopy techniques (scanning atomic force microscopy [11], scanning tunneling microscopy [12], and scanning near-field optical microscopy [13]), as well as methods involving scattering of an evanescent wave (for example, a surface plasmon) by the nanoparticle [14–16], are all based on the properties of the particle-surface interaction. This interaction is essential for certain kinds of heterogeneous catalysis [17,18]. The use of nanotechnologies in biological and medical applications has attracted attention to the interaction between biological objects and nanostructured surfaces [19–21]. Among possible applications that are currently discussed are various methods of the antiviral therapy, based on the interaction of viruses with nanoparticle preparations [22–24] and on the selective adsorption of viruses on a nanostructured surface [25]. Since the linear dimension of a virus is about 100 nm, the approximation of a pointlike particle becomes insufficient, and one has to take into account the local-field inhomogeneity when studying the interaction between the virus and a surface. This calls for the development of a theory of interaction between a nonpointlike particle and a surface.

The coupling between a particle (an atom, a molecule, or a nanoparticle) and a surface arises, particularly due to the van der Waals force combined with the short-range repulsive forces [26,27]. The adsorption potential defines such important properties as the type of adsorption and the adsorption isotherm [28,29]. There are numerous works (see, for example, Refs. [30–36]) devoted to the study of the interaction between a particle and an adsorbent surface. However, the effects of finite size and shape of the particle had not been taken

into account in a consistent way. Particularly, in the physical adsorption studies [30–34], usually only the attractive part of the adsorption potential has been calculated, while the analysis of the repulsive part has been overlooked.

It should be remarked that the problem of interaction between material objects caused by the quantum fluctuations of electromagnetic field has a long history, and has been studied in a wider context than the adsorption physics. It goes back to the works of Casimir and Polder [37,38] which predicted the emergence of an attractive interaction between two bodies, induced by vacuum fluctuations of the field. Subsequently, such forces induced by vacuum field fluctuations (known in the literature as the van der Waals, Casimir, and Casimir-Polder forces) have been studied by many authors (see, e.g., Refs. [39–51], and references therein). Particularly, Lifshitz, Dzyaloshinskii and Pitaevskii [39–42] have studied the interaction between two plates, and have shown that the van der Waals force between two bodies always has an attractive character and is monotonically decreasing with the increase of the distance between the bodies. Later, it was realized [43–45,47–51] that Casimir forces may acquire a repulsive character under special conditions, e.g., for a special system geometry [49,50], for a fine-tuned choice of the material constants of the interacting bodies and the medium they are immersed in [43,51], or when the interacting bodies are magnetic [45]. However, to our knowledge, in all those works the effects of nonlinearity were not taken into consideration. Particularly, the proof of a general theorem [46], prohibiting a repulsive Casimir force for pairs of objects connected by a mirror symmetry, implicitly assumes linearity of the problem.

It is well known that nanoparticles, metallic as well as nonmetallic, are usually characterized by a rather high nonlinear polarizability [52–55]. When a nanoparticle is located at a large distance from the surface, the linear polarizability plays a main role in the formation of the interaction potential. On the other hand, when a nanoparticle comes closer to the surface, the local field at the particle increases [56–58] and the nonlinearity starts to play an important role. At small distances from the surface, the nonlinear component presents the major contribution to the particle polarization, and the repulsive part of the interaction potential becomes strong. Thus, the importance of the local-field-enhancement effect makes it necessary to take into account the nonlinear polarization of

_____

*Corresponding author: v.lozovsk@gmail.com

the nanoparticle when the interaction between the nanoparticle and the surface is considered.

In Refs. [35,36], a self-consistent approach to the calculation of adsorption potential for *pointlike* objects (molecules) near a surface had been proposed, that allowed one to capture both the repulsive and the attractive parts of the interaction potential. The key ingredient of those works, responsible for the emergence of the repulsive component, was taking into account the nonlinear polarizability of the molecules. A realistic description of nanoparticle adsorption, however, requires going beyond the approximation of pointlike particles, which is known to result in strongly overestimated values of local-field intensities [59,60]. In a consistent description, effects of strongly inhomogeneous local-field distribution, together with shape effects, should play an important role. Thus, it is highly desirable to extend this approach to particles of a finite size, as the properties of nanoparticles are known to depend strongly on their linear dimensions and shape [61–64]. The proposed mechanism of generating the Casimir repulsion, based on nonlinearity, is obviously just one of many mechanisms that can contribute to the repulsive part of the potential, and in order to understand how important this mechanism can be for the nanoparticle adsorption, one needs to make realistic estimates taking into account the effects of size and shape of the particles.

In the present work, our goal is to construct a self-consistent theory for calculation of interaction potential between a finite-size nanoparticle and a flat surface of a solid, taking account of the nonlinear particle polarization. The theory is an extension of the approach developed previously in Refs. [35,36] for pointlike particles; it is constructed in the framework of the local-field method [59] and exploits the concept of effective susceptibility [65]. One should note that in contrast to numerous papers (see, for example, Ref. [66], and references therein) considering the microscopic theory of the adsorption potential, our work focuses on the general macroscopic properties governing the formation of the effective interaction between nonlinearly polarizing particles and solid surfaces. We show that the proposed approach leads to a qualitatively correct form of the particle-surface interaction, allowing one to obtain the interaction potential that contains a short-range repulsive core in addition to the long-range attraction. We perform numerical analysis that reveals a strong dependence of the interaction potential on the shape and size of the particle. Numerical estimates show that for typical nonlinearity strengths found in nanoparticles of semiconductor materials, our theory is applicable and yields binding energies consistent with the values characteristic for the physical adsorption. We study the particle-surface interaction in the presence of the propagating surface plasmon polariton, and show that the excitation of the surface wave leads to a sharp increase of the binding energy.

II. THE FREE ENERGY OF A NANOPARTICLE NEAR THE FLAT SOLID SURFACE

Consider a nanoparticle located close to the surface of a solid (Fig. 1). The particle, characterized by linear and nonlinear polarizabilities, is situated in the medium with the dielectric constant ε_m that fills the half space $z > 0$, at some distance d above the surface of the adsorbent with dielectric constant
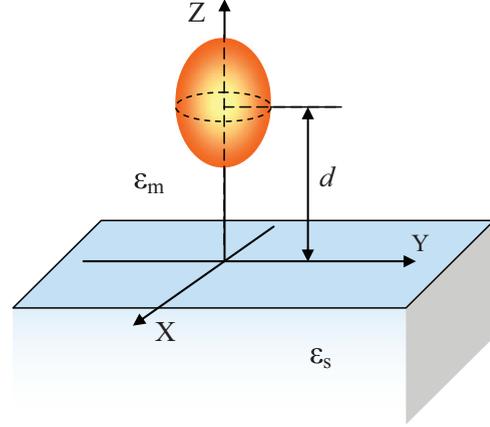
FIG. 1. (Color online) A nanoparticle near a flat surface.

ε_s (filling the other half space). The center of the particle is located at the point $\boldsymbol{R}_p = (0, 0, d)$. In order to find the relation between the polarization of the particle and the electric field acting on the system, one needs to calculate the free energy of the system, which can be written in the following form [67]:

$$F = \int_{V_p} d\boldsymbol{R}_p (U_{\text{int}} - P_i E_i) + \int_{\mathbb{R}^3} d\boldsymbol{R} \, W, \qquad (1)$$

where U_{int} is the internal energy density of the particle, $P_i E_i$ is the density of the energy of the dipole moment P_i interacting with electric field E_i, and W is the density of the field energy.

Assuming that the external electric field is much weaker than the intracrystalline field inside the particle, the contribution to the particle internal energy coming from the dipole moment induced inside the particle will be much smaller than the energy of the chemical bonds of the material. Then, keeping up to the quartic terms in the Taylor expansion of the internal energy in the polarization, one can write

$$U_{\text{int}}(\boldsymbol{P}) = U_0 + \frac{1}{2\varepsilon_0} (\alpha_{ij})^{-1} P_i P_j + \frac{1}{3\varepsilon_0} \sigma_{ijk} P_i P_j P_k$$
$$+ \frac{1}{4\varepsilon_0} \beta_{ijkl} P_i P_j P_k P_l. \qquad (2)$$

The first term in Eq. (2) represents the energy of the intraparticle chemical bonds, which does not depend on $\boldsymbol{P}$ and will be omitted in what follows. The term linear in $\boldsymbol{P}$ must vanish due to the requirement that the internal energy remains invariant when the particle rotates as a whole. The second term in Eq. (2) is the positively defined quadratic form, and α_{ij} is the tensor of linear polarizability of the particle. Tensors σ_{ijk} and β_{ijkl} describe the contributions of nonlinear effects to the particle polarizability. If the symmetry group of the particle contains a center of inversion, then tensor σ_{ijk} vanishes; in what follows, we will assume that this is the case. Taking into account the finite size of the particle under consideration, one can write the free energy of the system in the form

$$F = \int_{V_p} d\boldsymbol{R}_p \left[\frac{1}{2\varepsilon_0} (\alpha_{ij})^{-1} P_i(\boldsymbol{R}_p) P_j(\boldsymbol{R}_p) \right.$$
$$+ \frac{1}{4\varepsilon_0} \beta_{ijkl} P_i(\boldsymbol{R}_p) P_j(\boldsymbol{R}_p) P_k(\boldsymbol{R}_p) P_l(\boldsymbol{R}_p)$$
$$\left. - P_i(\boldsymbol{R}_p) E_i(P_i, \boldsymbol{R}_p) \right] + \int_{\boldsymbol{R}^3} d\boldsymbol{R} \frac{\varepsilon_m \varepsilon_0 E_i^2(P_i, \boldsymbol{R})}{2}, \qquad (3)$$

where the integration in the first term is over the particle volume V_p, while the second term describes the field energy and is represented as an integral over the entire space. In this expression $E_i(P_i, \boldsymbol{R}_p)$ is the local field acting on the particle. To find the ground state of the system, one should minimize its energy with respect to the dipole moments P_i [67–69]:

$$\delta F[P_i(\boldsymbol{R}_p)]|_{P_i(\boldsymbol{R}_p)} = 0. \tag{4}$$

To calculate the local field, it is convenient to use the Green's function method. The connection between the local field at an arbitrary point and the dipole moment density at the particle is expressed by the Lippmann-Schwinger equation [59,60,69],

$$E_i(\boldsymbol{R}) = E_i^{(0)}(\boldsymbol{R}) + \frac{k_0^2}{\varepsilon_0} \int_{V_p} d\boldsymbol{R}'_p G_{ij}(\boldsymbol{R}, \boldsymbol{R}'_p) P_j(\boldsymbol{R}'_p), \tag{5}$$

where $k_0 = \omega/c$ and c is the speed of light, $G_{ij}(\boldsymbol{R}, \boldsymbol{R}'_p)$ is the photon propagator (the electrodynamic Green's function) [63], and ω is the frequency of the local field (a summation over frequencies will be performed at a later stage). The explicit form of the photon propagator can be found in Refs. [59,70,71].

At this point a natural question arises, namely, what is the external field in Eq. (5)? According to the generally accepted opinion, the source of the van der Waals interaction [72,73] is the vacuum fluctuations of electromagnetic field. Then one should assume that $E_i^{(0)}(\boldsymbol{R})$ in Eq. (5) is the field of vacuum fluctuations playing the role of an external field to the system. Our aim is to express the dipole moment distribution inside the particle through the fluctuation field $E_i^{(0)}(\boldsymbol{R})$. On the other hand, fluctuations of the dipole moment inside the particle can also be the source of the interaction between the particle and a surface [72]. The dipole moment induces electric field in the substrate as well as in the particle. These fields, having a fluctuating nature, form the field at the particle which can be considered as "external" for the self-action processes inside of a nonpointlike particle and a substrate. One should note that the variation procedure is very complicated in the general case. To simplify the problem without loss of the generality, one can assume that tensors α_{ij} and β_{ijkl} are symmetric with respect to the permutation of the indices, and take into account that the Green's function $G_{ij}(\boldsymbol{R}, \boldsymbol{R}'_p)$ should satisfy the reciprocity theorem [73–76]. Substituting Eq. (5) into Eq. (3), one obtains

$$\begin{aligned}
F = \int_{V_p} d\boldsymbol{R}_p \bigg\{ &\frac{1}{2\varepsilon_0}(\alpha_{ij})^{-1} P_i(\boldsymbol{R}_p) P_j(\boldsymbol{R}_p) + \frac{1}{4\varepsilon_0}\beta_{ijkl} P_i(\boldsymbol{R}_p) P_j(\boldsymbol{R}_p) P_k(\boldsymbol{R}_p) P_l(\boldsymbol{R}_p) \\
&- P_i(\boldsymbol{R}_p) E_i^0(\boldsymbol{R}_p) - P_i(\boldsymbol{R}_p)\frac{k_0^2}{\varepsilon_0}\int_{V_p} d\boldsymbol{R}'_p G_{ij}(\boldsymbol{R}_p, \boldsymbol{R}'_p) P_j(\boldsymbol{R}'_p) \bigg\} \\
&+ \int_{\mathbb{R}^3} d\boldsymbol{R} \frac{1}{2}\varepsilon_m \varepsilon_0 \bigg\{ E_i^0(\boldsymbol{R}) + \frac{k_0^2}{\varepsilon_0}\int_{V_p} d\boldsymbol{R}'_p G_{ij}(\boldsymbol{R}, \boldsymbol{R}'_p) P_j(\boldsymbol{R}'_p) \bigg\}^2.
\end{aligned} \tag{6}$$

The minimization of the free energy yields the following equation for the polarization density $P_j(\boldsymbol{R}_p)$:

$$\begin{aligned}
&\frac{1}{\varepsilon_0}(\alpha_{ij})^{-1} P_j(\boldsymbol{R}_p) + \frac{1}{\varepsilon_0}\beta_{ijkl} P_j(\boldsymbol{R}_p) P_k(\boldsymbol{R}_p) P_l(\boldsymbol{R}_p) - E_i^0(\boldsymbol{R}_p) - \frac{k_0^2}{\varepsilon_0}\int_{V_p} d\boldsymbol{R}'_p G_{ij}(\boldsymbol{R}_p, \boldsymbol{R}'_p) P_j(\boldsymbol{R}'_p) \\
&+ \int_{\mathbb{R}^3} d\boldsymbol{R}\,\varepsilon_m k_0^2 G_{ij}(\boldsymbol{R}, \boldsymbol{R}_p) \bigg\{ E_j^0(\boldsymbol{R}) + \frac{k_0^2}{\varepsilon_0}\int_{V_p} d\boldsymbol{R}'_p G_{jl}(\boldsymbol{R}, \boldsymbol{R}'_p) P_l(\boldsymbol{R}'_p) \bigg\} = 0.
\end{aligned} \tag{7}$$

To obtain the ground state of the system, one should find from Eq. (7) the distribution of polarization in the particle as the function of the "external" field $E_i^{(0)}(\boldsymbol{R})$. To solve Eq. (7), one can use the method of successive approximations, under the assumptions that the free particle has no dipole moment and the fluctuating field is long range. We look for the solution in the form

$$P_i(\boldsymbol{R}_p) = P_i^{(0)}(\boldsymbol{R}_p) + P_i^{(1)}(\boldsymbol{R}_p) + \cdots, \tag{8}$$

which, as it will become clear below, is essentially a series in the small parameter, being the ratio of nonlinear and linear particle polarizabilities. In the zero-order approximation, the solution is obtained by setting the nonlinear polarizability to zero. Then the connection between the dipole moment and the external field is linear, $P_i^{(0)}(\boldsymbol{R}_p) = X_{ij}(\boldsymbol{R}_p) E_j^{(0)}(\boldsymbol{R}_p)$, where $X_{ij}(\boldsymbol{R}_p)$ is the effective susceptibility tensor of the particle. This leads to the following equation:

$$\begin{aligned}
&\frac{1}{\varepsilon_0}(\alpha_{ij})^{-1} X_{jl}(\boldsymbol{R}_p) E_l^{(0)}(\boldsymbol{R}_p) - \frac{k_0^2}{\varepsilon_0}\int_{V_p} d\boldsymbol{R}'_p G_{ij}(\boldsymbol{R}_p, \boldsymbol{R}'_p) X_{jl}(\boldsymbol{R}'_p) E_l^{(0)}(\boldsymbol{R}'_p) \\
&\quad + \int_{\mathbb{R}^3} d\boldsymbol{R}\,\varepsilon_m k_0^2 G_{ik}(\boldsymbol{R}, \boldsymbol{R}_p)\frac{k_0^2}{\varepsilon_0}\int_{V_p} d\boldsymbol{R}'_p G_{kj}(\boldsymbol{R}, \boldsymbol{R}'_p) X_{jl}(\boldsymbol{R}'_p) E_l^0(\boldsymbol{R}'_p) \\
&= E_i^{(0)}(\boldsymbol{R}_p) - \int_{\mathbb{R}^3} d\boldsymbol{R}\,\varepsilon_m k_0^2 G_{il}(\boldsymbol{R}, \boldsymbol{R}_p) E_l^{(0)}(\boldsymbol{R}).
\end{aligned} \tag{9}$$

At large distances $|\boldsymbol{R} - \boldsymbol{R}_p|$, the photon propagator $G_{ji}(\boldsymbol{R}, \boldsymbol{R}_p)$ falls off very fast (as $\sim 1/|\boldsymbol{R} - \boldsymbol{R}_p|^3$). Thus, in the last term of Eq. (9), the main contribution comes from $\boldsymbol{R}$ inside the volume of the particle and its immediate neighborhood. Because the linear dimension of the particle is supposed to be much smaller than the characteristic wavelength of the field of vacuum fluctuations, one can neglect the spatial dependence of $E_j^{(0)}(\boldsymbol{R})$ in the last term of Eq. (9):

$$\int_{\mathbb{R}^3} d\boldsymbol{R}\, \varepsilon_m k_0^2 G_{il}(\boldsymbol{R}, \boldsymbol{R}_p) E_l^{(0)}(\boldsymbol{R}) \approx \int_{\mathbb{R}^3} d\boldsymbol{R}\, \varepsilon_m k_0^2 G_{il}(\boldsymbol{R}, \boldsymbol{R}_p) E_l^{(0)}(\boldsymbol{R}_p). \tag{10}$$

Integrating both sides of Eq. (9) over the particle volume, and using Eq. (10), we obtain

$$\int_{V_p} d\boldsymbol{R}_p \left\{ \frac{1}{\varepsilon_0}(\alpha_{ij})^{-1} X_{jl}(\boldsymbol{R}_p) - \frac{k_0^2}{\varepsilon_0} \int_{V_p} d\boldsymbol{R}_p' G_{ij}(\boldsymbol{R}_p', \boldsymbol{R}_p) X_{jl}(\boldsymbol{R}_p) \right.$$

$$\left. + \int_{\mathbb{R}^3} d\boldsymbol{R}\, \frac{k_0^2}{\varepsilon_0} \int_{V_p} d\boldsymbol{R}_p' \varepsilon_m k_0^2 G_{ik}(\mathbf{R}, \boldsymbol{R}_p') G_{kj}(\mathbf{R}, \boldsymbol{R}_p) X_{jl}(\boldsymbol{R}_p) - \delta_{il} + \int_{\mathbb{R}^3} d\boldsymbol{R}\, \varepsilon_m k_0^2 G_{il}(\boldsymbol{R}, \boldsymbol{R}_p) \right\} E_l^{(0)}(\boldsymbol{R}_p) = 0. \tag{11}$$

Since the fluctuating field is, generally speaking, arbitrary and the integration in Eq. (11) is over the volume of the particle which may have any dimension and shape, one obtains the following expression for the effective susceptibility:

$$X_{jl}(\boldsymbol{R}_p) = \Omega_{ji}^{-1}(\boldsymbol{R}_p) \Lambda_{il}(\boldsymbol{R}_p), \tag{12}$$

with

$$\Lambda_{il}(\boldsymbol{R}_p) = \delta_{il} + \int d\boldsymbol{R}\, \varepsilon_m k_0^2 G_{il}(\boldsymbol{R}, \boldsymbol{R}_p), \tag{13}$$

and

$$\Omega_{ji}(\boldsymbol{R}_p) = \left[\frac{1}{\varepsilon_0}(\alpha_{ij})^{-1} - \frac{k_0^2}{\varepsilon_0} \int_{V_p} d\boldsymbol{R}_p' G_{ij}(\boldsymbol{R}_p', \boldsymbol{R}_p) + \int_{\mathbb{R}^3} d\boldsymbol{R}\, \frac{k_0^2}{\varepsilon_0} \int_{V_p} d\boldsymbol{R}_p' \varepsilon_m k_0^2 G_{ik}(\boldsymbol{R}, \boldsymbol{R}_p') G_{kj}(\boldsymbol{R}, \boldsymbol{R}_p) \right]. \tag{14}$$

Equations (12)–(14) complete the calculation of the zero-order polarization $P_i^{(0)}(\boldsymbol{R}_p) = X_{ij}(\boldsymbol{R}_p) E_j^{(0)}(\boldsymbol{R}_p)$.

The first-order correction $P_j^{(1)}(\boldsymbol{R})$ is determined by the following equation:

$$\frac{1}{\varepsilon_0}(\alpha_{ij})^{-1} P_j^{(1)}(\boldsymbol{R}_p) + \frac{1}{\varepsilon_0} \beta_{ijkl} P_j^{(0)}(\boldsymbol{R}_p) P_k^{(0)}(\boldsymbol{R}_p) P_l^{(0)}(\boldsymbol{R}_p) - \frac{k_0^2}{\varepsilon_0} \int_{V_p} d\boldsymbol{R}_p' G_{ij}(\boldsymbol{R}_p, \boldsymbol{R}_p') P_j^{(1)}(\boldsymbol{R}_p')$$

$$+ \int_{\mathbb{R}^3} d\boldsymbol{R}\, \varepsilon_m k_0^2 G_{ij}(\boldsymbol{R}, \boldsymbol{R}_p) \frac{k_0^2}{\varepsilon_0} \int_{V_p} d\boldsymbol{R}_p' G_{jl}(\boldsymbol{R}, \boldsymbol{R}_p') P_l^{(1)}(\boldsymbol{R}_p') = 0. \tag{15}$$

This integral equation can be considerably simplified if we take into account that the propagator is strongly peaked at the point where its two arguments are equal, and assume that the peak width is small compared to the characteristic scale of the spatial variation of $P_j^{(1)}(\boldsymbol{R})$. Then, to a good approximation, the correction $P_j^{(1)}(\boldsymbol{R})$ in the last two terms of Eq. (15) can be replaced by its value at the peak of the propagator and thus taken out of the integral, and we obtain

$$\left[(\alpha_{ij})^{-1} - k_0^2 \int_{V_p} d\boldsymbol{R}_p' G_{ij}(\boldsymbol{R}_p, \boldsymbol{R}_p') + \int_{\mathbb{R}^3} d\boldsymbol{R}\, \varepsilon_m k_0^2 G_{il}(\boldsymbol{R}, \boldsymbol{R}_p) k_0^2 \int_{V_p} d\boldsymbol{R}_p' G_{lj}(\boldsymbol{R}, \boldsymbol{R}_p') \right] P_j^{(1)}(\boldsymbol{R}_p)$$

$$+ \beta_{ijkl} P_j^{(0)}(\boldsymbol{R}_p) P_k^{(0)}(\boldsymbol{R}_p) P_l^{(0)}(\boldsymbol{R}_p) = 0. \tag{16}$$

This yields the first-order correction to the particle polarization in the following form:

$$P_j^{(1)}(\boldsymbol{R}_p) = \mathcal{A}_{jsmn}(\boldsymbol{R}_p) E_s^{(0)}(\boldsymbol{R}_p) E_m^{(0)}(\boldsymbol{R}_p) E_n^{(0)}(\boldsymbol{R}_p), \tag{17}$$

where

$$\mathcal{A}_{jsmn}(\boldsymbol{R}_p) = -\alpha_{ji} \tilde{\beta}_{irkl} X_{rs}(\boldsymbol{R}_p) X_{km}(\boldsymbol{R}_p) X_{ln}(\boldsymbol{R}_p), \tag{18}$$

with the renormalized nonlinear polarizability

$$\tilde{\beta}_{irkl} = \left[\delta_{vi} - \frac{k_0^2}{\varepsilon_0} \int_{V_p} d\boldsymbol{R}_p' G_{vn}(\boldsymbol{R}_p, \boldsymbol{R}_p') \alpha_{ni} + \int_{\mathbb{R}^3} d\boldsymbol{R}\, \varepsilon_m k_0^2 G_{vl}(\boldsymbol{R}, \boldsymbol{R}_p) \frac{k_0^2}{\varepsilon_0} \int_{V_p} d\boldsymbol{R}_p' G_{ln}(\boldsymbol{R}, \boldsymbol{R}_p') \alpha_{ni} \right]^{-1} \beta_{vrkl}. \tag{19}$$

It is worth noting that Eq. (19) indicates the possibility of increasing substantially the nonlinear polarizability of a nanoparticle due to the local-field enhancement. A detailed study of the influence of the local-field effects on the nonlinear polarizability of nanoparticles is, however, outside the main focus of the present work, so we will not dwell on it in any detail here.

As a result, one obtains the following connection between the dipole moment at the particle and the fluctuating field, in the lowest approximation in the nonlinearity coefficient β:

$$
\begin{aligned}
P_j(\boldsymbol{R}_p) = {} & X_{jl}(\boldsymbol{R}_p)E_l^{(0)}(\boldsymbol{R}_p) \\
& + \mathcal{A}_{jsmn}(\boldsymbol{R}_p)E_s^{(0)}(\boldsymbol{R}_p)E_m^{(0)}(\boldsymbol{R}_p)E_n^{(0)}(\boldsymbol{R}_p), \quad (20)
\end{aligned}
$$

with the effective linear $X_{jl}(\boldsymbol{R}_p)$ and nonlinear $\mathcal{A}_{jsmn}(\boldsymbol{R}_p)$ polarizabilities given by Eqs. (12) and (18), respectively. Now, having established the solution for the particle polarization, we have all the necessary information for calculating the potential of interaction between the particle and the surface.

III. THE INTERACTION POTENTIAL

The total energy of the system in the presence of the fluctuating field of frequency ω, having the sense of an interaction potential, can be defined as [73]

$$
U(d,\omega) = - \int_{V_p} d\boldsymbol{R}_p\, P_j E_j - \delta U_\infty, \quad (21)
$$

where d is the distance between the particle and the surface of adsorbent, and the last term

$$
\delta U_\infty = - \int_{V_p} d\boldsymbol{R}_p\, P_j E_j \bigg|_{d\to\infty}, \quad (22)
$$

denotes the energy of the system when the particle is pulled away from the surface to the infinity. To calculate the electric field, one has to substitute the relation (20), connecting the external field with the induced dipole moment, into the integral in the Lippmann-Schwinger equation (5). Then, the electric field at the particle can be expressed as

$$
\begin{aligned}
E_j(\boldsymbol{R}_p) = {} & E_j^{(0)}(\boldsymbol{R}_p) + \mathcal{L}_{jk}(\boldsymbol{R}_p)E_k^{(0)}(\boldsymbol{R}_p) \\
& + \mathcal{N}_{jsmn}(\boldsymbol{R}_p)E_s^{(0)}(\boldsymbol{R}_p)E_m^{(0)}(\boldsymbol{R}_p)E_n^{(0)}(\boldsymbol{R}_p), \quad (23)
\end{aligned}
$$

where

$$
\mathcal{L}_{jk}(\boldsymbol{R}_p) = \frac{k_0^2}{\varepsilon_0} \int_{V_p} d\boldsymbol{R}_p'\, G_{ji}(\boldsymbol{R}_p,\boldsymbol{R}_p')X_{il}(\boldsymbol{R}_p'), \quad (24)
$$

$$
\mathcal{N}_{jsmn}(\boldsymbol{R}_p) = \frac{k_0^2}{\varepsilon_0} \int_{V_p} d\boldsymbol{R}_p'\, G_{ji}(\boldsymbol{R}_p,\boldsymbol{R}_p')\mathcal{A}_{ismn}(\boldsymbol{R}_p'). \quad (25)
$$

Then, substituting Eqs. (20) and (23) into Eq. (21), one obtains the interaction potential

$$
\begin{aligned}
U(d,\omega) = {} & \Im_{jl}(d)E_l^{(0)}(\boldsymbol{R}_p)E_j^{(0)}(\boldsymbol{R}_p) \\
& + \Re_{lsmn}(d)E_l^{(0)}(\boldsymbol{R}_p)E_s^{(0)}(\boldsymbol{R}_p)E_m^{(0)}(\boldsymbol{R}_p)E_n^{(0)}(\boldsymbol{R}_p), \\
& \hspace{10.5cm} (26)
\end{aligned}
$$

where

$$
\Im_{lk}(d) = - \int_{V_p} d\boldsymbol{R}_p\, X_{lk}(\boldsymbol{R}_p) - \int_{V_p} d\boldsymbol{R}_p\, X_{lj}(\boldsymbol{R}_p)\mathcal{L}_{jk}(\boldsymbol{R}_p), \quad (27)
$$

$$
\begin{aligned}
\Re_{ismn}(d) = {} & - \int_{V_p} d\boldsymbol{R}_p\, X_{ij}(\boldsymbol{R}_p)\mathcal{N}_{jsmn}(\boldsymbol{R}_p) \\
& - \int_{V_p} d\boldsymbol{R}_p\, \mathcal{A}_{ismn}(\boldsymbol{R}_p) \\
& - \int_{V_p} d\boldsymbol{R}_p\, \mathcal{L}_{ik}(\boldsymbol{R}_p)\mathcal{A}_{ksmn}(\boldsymbol{R}_p). \quad (28)
\end{aligned}
$$

The first term in Eq. (26) is determined solely by the linear response, while the second term stems from the finite nonlinear polarizability.

Further, to obtain the physical interacting potential, one has to perform the statistical averaging of Eq. (28) over the vacuum fluctuations of the electric field [72,73]. The calculation of the physical interaction potential thus involves computing fluctuation field correlators $\langle E_i^{(0)}(\boldsymbol{R}_p)E_j^{(0)}(\boldsymbol{R}_p)\rangle_\omega$ and $\langle E_i^{(0)}(\boldsymbol{R}_p)E_j^{(0)}(\boldsymbol{R}_p)E_k^{(0)}(\boldsymbol{R}_p)E_l^{(0)}(\boldsymbol{R}_p)\rangle_\omega$. We use the random phase approximation, which allows one to express four-point correlators through two-point ones [77,78]:

$$
\begin{aligned}
& \langle E_i^{(0)}(\boldsymbol{R}_p)E_j^{(0)}(\boldsymbol{R}_p)E_k^{(0)}(\boldsymbol{R}_p)E_l^{(0)}(\boldsymbol{R}_p)\rangle_\omega \\
& \approx \sum_{\mathrm{Perm}(i,j,k,l)} \langle E_i^{(0)}(\boldsymbol{R}_p)E_j^{(0)}(\boldsymbol{R}_p)\rangle_\omega \langle E_k^{(0)}(\boldsymbol{R}_p)E_l^{(0)}(\boldsymbol{R}_p)\rangle_\omega,
\end{aligned}
$$
$$
(29)
$$

where the summation is over all possible permutations of the indices. Because of the homogeneity and isotropy of the vacuum state, the correlator $\langle E_i^{(0)}(\boldsymbol{R}_p)E_j^{(0)}(\boldsymbol{R}_p)\rangle_\omega$ should be proportional to the unit tensor δ_{ij} [73]. Then, one can express the spectral density of the correlator as

$$
\langle E_i^{(0)}(\boldsymbol{R}_p)E_j^{(0)}(\boldsymbol{R}_p)\rangle_\omega = \tfrac{2}{3}\hbar(\omega/c)^3 \delta_{ij}\,\mathrm{sgn}(\omega), \quad (30)
$$

where sgn is the signum function. This result is valid in the framework of the near-field approximation (when the retardation processes are neglected); that is, $\omega \ll c/R$.

It should be noted that the van der Waals interaction arises due to fluctuations of dipole moments inside the particle as well as due to the vacuum fluctuations of the electromagnetic field [72,73]. In the self-consistent approach developed here, these two mechanisms are described by the external (with respect to the particle) field, which can represent both the field of vacuum fluctuations and the field induced by fluctuations of the dipole moment inside the particle. Since all electromagnetic field correlators are defined by the medium in which the field propagates, we suppose that correlators of both fields (the field of vacuum fluctuations and the field induced by dipole moment fluctuations) can be expressed via the electrodynamic Green's function of the medium in which the particle is situated.

To find the final expression for the interaction energy, one has to integrate the averaged spectral component of the energy

(26) over the entire frequency range,

$$U(d) = \int_0^\infty \langle U(d,\omega) \rangle_\omega f(\omega) d\omega, \qquad (31)$$

using the Bose distribution function for virtual photons,

$$f(\omega) = \frac{1}{e^{\hbar\omega/kT} - 1}. \qquad (32)$$

With the help of Eqs. (26)–(32), one can compute the potential of interaction between the adsorbent and the particle for any geometry of the problem.

IV. NUMERICAL ANALYSIS OF THE ADSORPTION POTENTIAL PROPERTIES

To illustrate the approach developed above, and to show some important properties of the adsorption potential, we apply our theoretical scheme to calculate the interaction potential for the sufficiently general case of an ellipsoidal particle. Taking into account the range of the distances involved and assuming that the adsorbent particle has a nanometer-scale size, the photon propagator can be approximated by its near-field contribution [59,70,71]. In this approximation, the direct part of the propagator takes the form

$$D_{ij}(\mathbf{r},\mathbf{r}',\omega) = \frac{1}{4\pi}\left[\frac{c^2}{\omega^2 R^3}\delta_{ij} - \frac{3c^2}{\omega^2 R^3}\mathbf{e}_R\mathbf{e}_R \right], \qquad (33)$$

where $R = |\mathbf{r} - \mathbf{r}'|$ and $\mathbf{e}_R = \mathbf{R}/R$, while the indirect part is given by

$$I_{ij}(\mathbf{R},\mathbf{R}',\omega) = D_{il}(\mathbf{R},\mathbf{R}'_M,\omega)M_{lj}(\omega), \qquad (34)$$

$$M_{lj}(\omega) = \frac{\varepsilon_s(\omega) - \varepsilon_m}{\varepsilon_s(\omega) + \varepsilon_m}\begin{pmatrix} -1 & 0 & 0 \\ 0 & -1 & 0 \\ 0 & 0 & 1 \end{pmatrix}. \qquad (35)$$

$\mathbf{R}'_M = (x',y',-z')$ and $\varepsilon_s(\omega)$ is the dielectric constant of the adsorbent. The medium is supposed to be vacuum (or air) characterized by the dielectric constant $\varepsilon_m = 1$.

For a fixed particle shape, and fixed values of the dielectric constants, the shape of the interaction potential depends only on the ratio $\tilde{\beta}/\alpha$ of nonlinear and linear polarizabilities. For numerical estimates throughout this section, we have set this ratio to be $\tilde{\beta}/\alpha = 2.13 \times 10^{-10}$ erg^{-2}. This corresponds to the known value of the third-order nonlinear susceptibility for Si [79]. The dependence of the properties of the interaction potential on $\tilde{\beta}$ will be discussed later in Sec. VI.

It has to be noted that, according to Eq. (20), the nonlinear polarizability $\tilde{\beta}$ is renormalized by local-field effects, so it differs from the "bare" nonlinear polarizability β and, generally speaking, depends on the shape and dimension of the particle. For numerical estimates below, we use the experimental data for $\tilde{\beta}$ obtained for nanoparticles.

Further, as follows from Eqs. (31)–(35), the interaction potential is affected by the frequency dependence of the particle susceptibility and of the dielectric constant of the substrate. Since the main focus of our work is to demonstrate the effect of the nonlinear polarizability leading to the formation of the repulsive part of the potential, we did not aim at making quantitative estimates for specific materials. At not too high

temperatures the main contribution to the integral in Eq. (31) comes from low frequencies, so in our numerical analysis we have used the low-frequency values of the dielectric constants of both the nanoparticle and the adsorbent. At the same time, according to Eq. (12), the particle susceptibility, characterizing its linear response to an external field, remains frequency dependent. We note that a similar procedure has been used in Ref. [73] (Chap. 2, pp.23–32) for the estimate of the van der Waals potential of interaction between two particles, and it has been shown that the formula for the potential can be expressed through the static polarizabilities of the constituent materials. Such a calculation, of course, neglects the peculiarities of the dispersion curves of real materials, but still leads to the results that are *qualitatively* correct.

The results of our calculations, for different particle shapes and different relations between the dielectric constants of the particle, the adsorbent, and the medium, are presented in Figs. 2–6. The analysis of those results allows one to reach several conclusions on the properties of the adsorption potential:

(i) The interaction potential at large distances between the particle and the surface is attractive, and becomes repulsive at short distances;

(ii) The interaction potential strongly depends on the material of the nanoparticle;

(iii) The interaction potential strongly depends on the shape and dimensions of the particle.

The dependence of the interaction potential on dielectric constants of the particle and substrate is shown in Fig. 2. One can see that the binding energy increases monotonically with the increase of the dielectric constant of the particle material (with the same adsorbent). The position of the minimum of the interaction potential depends on the coefficient of nonlinearity (see the estimates for the applicability range of the theory in Sec. VI). One should note that the spatial position of the potential minimum (the equilibrium distance) depends on the dielectric constant of the substrate and increases with the decrease of the dielectric constant.

The dependences of the normalized force and the interaction potential on the particle dimensions and on the distance to the surface are shown in Fig. 3. In atomic force microscopy (AFM) experiments it is common to present the properties of the dispersion interaction as a graph of the interaction force F normalized by the particle radius R_p. Our results for the form of the curves describing the dependence of F/R_p on the distance to the surface d, shown in Fig. 3(a), as well as the characteristic distances at which the repulsive nature of the interaction becomes pronounced, qualitatively agree with the results of Ref. [80] where long-range repulsive forces between a nanoparticle and a surface have been studied by means of AFM.

Figure 3(b) shows that the minimum of the potential is formed at the distance roughly corresponding to the linear dimension of the particle. Particles of larger radius have deeper minima of the interaction potential (i.e., larger binding energy). Indeed, in the framework of the point dipole approximation, the interaction potential is proportional to the total dipole moment induced at the particle, which depends on the particle radius as $\sim R^3$. In our approach, effects of finite size are taken into account. These effects lead to inhomogeneity of the local field
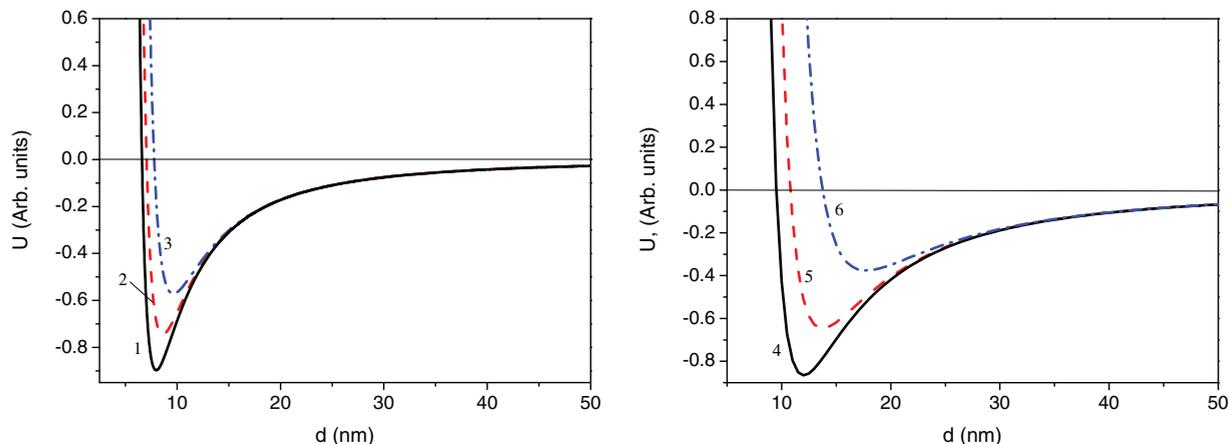
FIG. 2. (Color online) The interacting potential for a spherical particle with the radius $R_p = 5$ nm. Different curves correspond to different values of the dielectric constants of the adsorbent (ε_s) and the particle (ε_p). Curves 1–3 in the left panel correspond to $\varepsilon_s = 3$ and $\varepsilon_p = 20$ (curve 1), $\varepsilon_p = 16$ (curve 2), $\varepsilon_p = 11.8$ (curve 3). Curves 4–6 in the right panel correspond to $\varepsilon_s = 1.5$ and $\varepsilon_p = 16$ (curve 4), $\varepsilon_p = 11.8$ (curve 5), and $\varepsilon_p = 7$ (curve 6).

inside the particle that plays a prominent role in the formation of the interaction potential. Due to this inhomogeneity, the dependence of the interaction potential on the particle radius becomes slightly weaker than R^3. This leads to a nearly size-independent depth of the potential normalized per particle volume.

As mentioned above, the interaction potential strongly depends on the particle shape, which is illustrated in Fig. 4 Specifically, calculations of interaction potential for nanoparticles of oblate ellipsoidal shape (with semiprincipal axes $h_x = h_y$, and different values of the ratio $h_z/h_x < 1$), with the fixed particle volume equal to that of a sphere with the radius of 10 nm show that the interaction potential has a deeper minimum for the particles with smaller ratio h_z/h_x. The minimum of the potential forms at the distance about the linear dimension of the particle, which becomes smaller for a smaller ratio h_z/h_x. The same calculations of interaction potential for nanoparticles of prolate ellipsoidal shape (ratio

$h_z/h_x > 1$) show that in this case the depth of the potential minimum is smaller than for the case of oblate ellipsoids. This depth decreases with the increase of h_z/h_x. The distance at which the potential minimum is formed is larger in this case and increases with the increasing ratio h_z/h_x.

One can see that the interaction potential strongly depends on the shape and dimension of the particle. Namely, the interaction between oblate particles and the adsorbent is stronger than in the case of prolate particles, which can be explained by the higher polarizability of oblate ellipsoids near a flat surface in comparison to prolate ellipsoids made of the same material. The minimum of the potential is located at the distance of about the smallest linear dimension of the particle (so this distance is smaller in the case of oblate ellipsoids). When the particle shape changes from oblate to prolate ellipsoid at fixed volume, the potential with a deep minimum characteristic for oblate particles transforms smoothly into the potential with a shallow minimum typical for prolate particles.
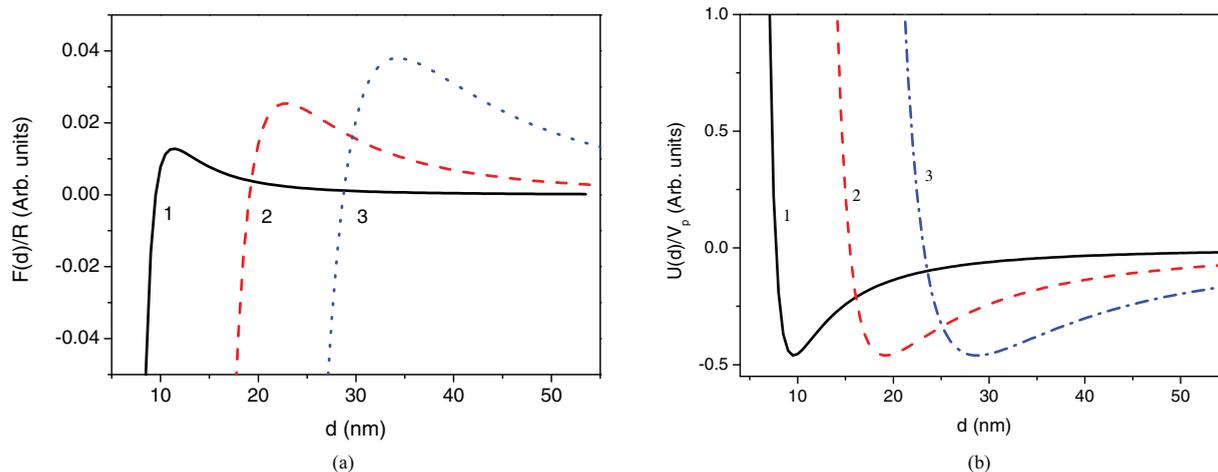
FIG. 3. (Color online) (a) Normalized force ($F(d)/R$). (b) Normalized interacting potential [$U(d)/V_p$, where V_p is the particle volume] for a spherical particle ($\varepsilon_p = 11.8$) at the adsorbent ($\varepsilon_s = 3$), for different values of the particle radius: $R_p = 5$ nm (curve 1), $R_p = 10$ nm (curve 2), $R_p = 15$ nm (curve 3).
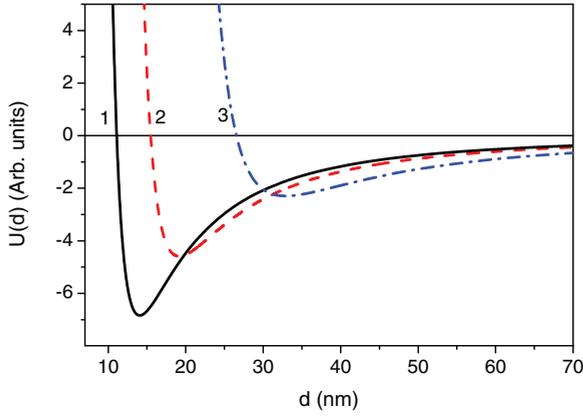
FIG. 4. (Color online) Interaction potential for nanoparticles of ellipsoidal shape (with semiprincipal axes $h_x = h_y$, with the fixed particle volume equal to that of a sphere with the radius of 10 nm, for an oblate ellipsoid (curve 1, $h_z/h_x = 1/2$, $h_x \approx 12.6$ nm), a sphere (curve 2), and a prolate ellipsoid (curve 3, $h_z/h_x = 2$, $h_x \approx 7.93$ nm). The dielectric constant of the particle is $\varepsilon_p = 11.8$ and that of the adsorbent is $\varepsilon_s = 3$.

V. THE ADSORPTION POTENTIAL IN THE PRESENCE OF A SURFACE PLASMON POLARITON PROPAGATING ALONG THE INTERFACE

Let us consider the case when a nanoparticle interacts with a metallic surface in the presence of a propagating surface plasmon polariton. To find the interaction potential in this case, one should calculate the appropriate form of the indirect part of the Green's function describing the metallic substrate along which the surface plasmon polariton is propagating. The explicit form of the Green's function in the so-called k-z representation is [81]

$$
I_{ij}(k,z,z',\omega)
$$
$$
= 2\pi i\, e^{i\beta_1(z+z')}
\begin{pmatrix}
(\beta_1/\varepsilon_m)\boldsymbol{R}_p & 0 & k\mathrm{R}_p \\
0 & (k_0^2/\beta_1)R_s & 0 \\
-k\mathrm{R}_p & 0 & -(k^2/\beta_1)\boldsymbol{R}_p
\end{pmatrix},
$$
(36)

where z is the coordinate of the field source plane, z' is the coordinate of the plane containing the observation point, $\boldsymbol{R}_p = \frac{\beta_2 - \varepsilon_s \beta_1}{\beta_2 + \varepsilon_s \beta_1}$ and $R_s = \frac{\beta_1 - \beta_2}{\beta_1 + \beta_2}$ are the Fresnel reflection coefficients for p- and s-polarized light, respectively, and

$$
\beta_1 = \sqrt{k_0^2 - k^2}, \tag{37}
$$

$$
\beta_2 = \sqrt{\varepsilon_s k_0^2 - k^2}. \tag{38}
$$

To use the method developed in this work, one should find the form of the Green's function in the coordinate space. Performing the Fourier transformation over the in-plane coordinates, one obtains [81]

$$
\bar{\mathcal{J}}_{ij}(x,x',y,y',z,z',\omega)
$$
$$
= \frac{1}{(2\pi)^2} \int_0^\infty 2\pi i\, e^{i\beta_1(z+z')} I_{ij}(k,z,z',\omega) e^{-i\mathbf{k}\cdot(\mathbf{r}-\mathbf{r}')} d^2k, \tag{39}
$$

where $\mathbf{r} = (x,y)$ is the coordinate of the observation point and $\mathbf{r}' = (x',y')$ is the coordinate of the point of field source location. To calculate the Green's function $\bar{\mathcal{J}}_{ij}(x,x',y,y',z,z',\omega)$ in an arbitrary Cartesian coordinate system, one can rotate the initial coordinate system (in which the x axis is set along the direction of the wave vector $\boldsymbol{k}$) around the z axis, which is achieved by the rotation matrix

$$
S_{ij} =
\begin{pmatrix}
\cos\alpha & \sin\alpha & 0 \\
-\sin\alpha & \cos\alpha & 0 \\
0 & 0 & 1
\end{pmatrix}, \tag{40}
$$

α being the angle between the $\boldsymbol{R}$ and $\boldsymbol{k}$ axes. The Green's function in a new coordinate system (with the x axis along the direction given by the vector $\boldsymbol{R} = \boldsymbol{r} - \boldsymbol{r}'$, and the z axis coinciding with that of the "old" coordinate system) takes the form

$$
\mathcal{J}_{ij} = S_{ik}^{-1} \cdot \bar{\mathcal{J}}_{kl} \cdot S_{lj}. \tag{41}
$$

Explicitly, this yields

$$
\mathcal{J}_{ij}(R,z,z') = \frac{1}{(2\pi)^2} \int_0^{2\pi} d\alpha \int_0^\infty q_{ij}(k,\alpha,z,z') e^{-ikR\cos\alpha} k\,dk, \tag{42}
$$

where

$$
q_{ij}(k,\alpha,z,z') =
\begin{pmatrix}
I_{11}\cos^2\alpha + I_{22}\sin^2\alpha & (I_{11} - I_{22})\sin\alpha\cos\alpha & I_{13}\cos\alpha \\
(I_{11} - I_{22})\sin\alpha\cos\alpha & I_{11}\sin^2\alpha + I_{22}\cos^2\alpha & I_{13}\sin\alpha \\
I_{31}\cos\alpha & I_{31}\sin\alpha & I_{33}
\end{pmatrix}. \tag{43}
$$

Performing the integration over the polar angle α, one obtains

$$
\mathcal{J}_{ij}(R,z,z')
$$
$$
= \frac{1}{4\pi} \int_0^\infty k\,dk
$$
$$
\times
\begin{pmatrix}
I_{11}(k)[J_0(\mu) - J_2(\mu)] + I_{22}(k)[J_0(\mu) + J_2(\mu)] & 0 & 2i\,I_{13}(k)J_1(\mu) \\
0 & I_{11}(k)[J_0(\mu) + J_2(\mu)] + I_{22}(k)[J_0(\mu) - J_2(\mu)] & 0 \\
2i\,I_{31}(k)J_1(\mu) & 0 & 2I_{33}(k)J_0(\mu)
\end{pmatrix}, \tag{44}
$$

where $J_n(\mu)$ is the Bessel function of the first kind, and $\mu = kR$.

It is instructive to split the integral over the wave vector k as follows:

$$\int_0^\infty (\cdots)dk = \int_0^{k_0} (\cdots)dk + \int_{k_0}^\infty (\cdots)dk. \qquad (45)$$

The first term on the right-hand side of Eq. (43) is associated with the field modes which propagate without decay, which follows from the fact that $\beta_1 > 0$ for $k < k_0$, while the second term is related to the exponentially decaying field modes. Following Ref. [81], one can calculate the contribution to $\mathcal{J}_{ij}$ from the decaying modes via contour integration in the complex **k** plane. By the contour integration one picks up the contribution from the pole at $k = k_{\text{surf}}$, where the pole location is determined by the dispersion relation of the surface plasmon polariton [82],

$$\beta_2(k_{\text{surf}},\omega) + \varepsilon_s(\omega)\beta_1(k_{\text{surf}},\omega) = 0. \qquad (46)$$

Since $I_{11}(k,\omega)$, $I_{13}(k,\omega)$, $I_{31}(k,\omega)$, and $I_{33}(k,\omega)$ all have a pole in k (when $\varepsilon_s < 0$), all the tensor components of $\mathcal{J}_{ij}(R,z,z')$ contain the corresponding contributions. Since the main contribution to the integral over the decaying modes stems from the pole, in the further analysis we use the approximation

$$\int_0^\infty (\cdots)dk = \int_0^{k_0} (\cdots)dk + 2\pi i \text{Res}(k_{\text{surf}}), \qquad (47)$$

where $\text{Res}(k_{\text{surf}})$ denotes the value of the residue at the pole. Using Eqs. (37) and (38), from the pole condition in Eq. (46) one obtains the well-known dispersion relation for surface polaritons on a flat surface [82]:

$$k_{\text{surf}} = k_0 \sqrt{\frac{\varepsilon_s}{1 + \varepsilon_s}}. \qquad (48)$$

A straightforward computation of the pole contributions to the integral in Eq. (44) yields the following expression for Green's tensor [81]

$$\mathcal{J}_{ij}(R,\omega) = 4\pi e^{-\frac{\varepsilon_m k_0(z+z')}{(\varepsilon_m+\varepsilon_s)^{1/2}}} \frac{k_0^3(\varepsilon_m\varepsilon_s)^2}{(\varepsilon_m+\varepsilon_s)^{3/2}(\varepsilon_m^2+\varepsilon_s^2)} \begin{pmatrix} \frac{J_0(\mu_{\text{surf}})+J_2(\mu_{\text{surf}})}{2} & 0 & i\sqrt{\varepsilon_p\varepsilon_s}J_1(\mu_{\text{surf}}) \\ 0 & \frac{J_0(\mu_{\text{surf}})+J_2(\mu_{\text{surf}})}{2} & 0 \\ -i\sqrt{\varepsilon_p\varepsilon_s}J_1(\mu_{\text{surf}}) & 0 & -\varepsilon_p\varepsilon_s J_0(\mu_{\text{surf}}) \end{pmatrix}, \qquad (49)$$

where $\mu_{\text{surf}} = k_{\text{surf}} R$.

Using the above equation for the indirect part of the Green's function, we have computed the interaction potential for the case of an excited surface wave. The results of this calculation, in comparison to the case of the interface without excitations, are shown in Fig. 5. As one can see, the excitation of surface wave leads to a drastic enhancement of the particle-surface interaction. Particularly, in the case considered here, the adsorption energy increases up to ten times when the surface plasmon polariton is excited.
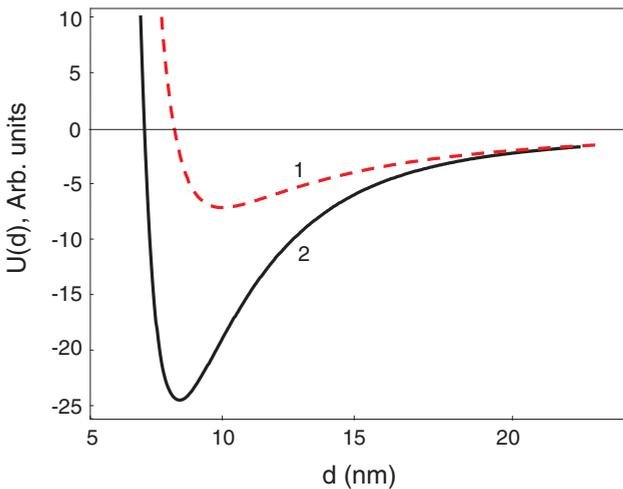
FIG. 5. (Color online) The interaction potential for a spherical particle of the radius $r = 5$ nm at a "free" golden surface (curve 1) and in the presence of a propagating surface plasmon polariton (curve 2).

VI. SUMMARY AND DISCUSSION

We have presented a theoretical approach for calculating the interaction between a finite-size nanoparticle of an arbitrary shape and the surface of a solid. Our method is rather general since it is based on macroscopic electrodynamics (specifically, it is constructed in the framework of the self-consistent local-field method [59] and exploits the concept of effective susceptibility [60]) and does not depend on the microscopic details of the problem. One of the key points of our approach is the account taken of the nonlinear component of the particle polarization; the necessity of doing this is dictated by the strong local-field enhancement which takes place at small distances between the particle and the surface. Our theory is a generalization of the approach of Refs. [35,36] to the case of finite-size particles. We show that the proposed approach allows one to obtain the interaction potential that contains both short-range repulsion and the long-range attraction, thus yielding an adequate description of the adsorption physics. Our numerical analysis for the case of ellipsoid-shaped particles shows that the interaction potential strongly depends on the geometry (shape and size) of the particle.

The main feature of the particle-surface interaction potential in our approach is the presence of the repulsive part, which is naturally caused by the finite nonlinear polarizability of the particle. The repulsive part is generated due to the contribution in the energy proportional to the fourth power of the particle polarization. It is thus clear that the repulsion generated by the above mechanism will substantially depend on the strength of nonlinearity, and will be negligible in the limit of extremely weak nonlinearity. Here a natural question arises, namely, what are the values of the nonlinearity strength that are necessary
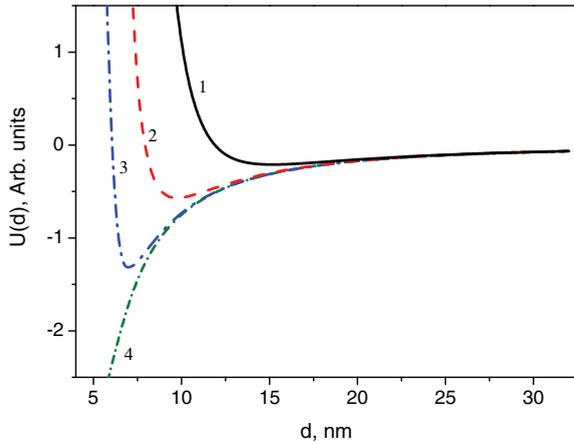
FIG. 6. (Color online) Dependence of the interaction potential on the dimensionless nonlinear polarizability $b = \tilde{\beta}/(\alpha C)$, $C = 2.13 \times 10^{-6}$ erg^{-2}, for a spherical nanoparticle of 5 nm radius. Curves 1–4 correspond to the values $b = 10^{-3}$, 10^{-4}, 10^{-5}, 10^{-6}, respectively. The dielectric constants of the adsorbent (ε_s) and the particle (ε_p) are set to $\varepsilon_s = 3$ and $\varepsilon_p = 11.8$.

for the proposed mechanism to work, and how are those values related to the typical parameters of real materials.

To analyze the dependence of the interaction potential on the nonlinearity strength, it is convenient to introduce the dimensionless nonlinearity parameter $b = \tilde{\beta}/(\alpha C)$, where $C = 2.13 \times 10^{-6}$ erg^{-2} is chosen in a such way that $b = 10^{-4}$ corresponds to the known values of nonlinearity in silicon [79,83]. In Fig. 6, we illustrate the change of the typical shape of the interaction potential with the decrease of the parameter b, for some hypothetic nanoparticle of 5 nm radius. One can see that, as expected, the decrease of nonlinearity leads to a shift of the potential minimum to the region of small distances, and ultimately leads to a complete disappearance of the repulsive part. One can conclude that in the case shown in Fig. 6, the nonlinear mechanism of the "Casimir repulsion" works for sufficiently large nonlinearity values $b \geqslant 10^{-5}$, when the potential minimum forms at distances larger than the particle radius, and the short-range repulsion due to chemical bonds between the particle and the adsorbent surface can be neglected. It is worthwhile to note that the actual nonlinearity strength in silicon nanoparticle $b = 10^{-4}$, falls within this range where our theory is applicable; moreover, in this case the binding energy can be estimated as $U_{\max} \sim 0.04$ eV, which is consistent with the typical values of the binding energy in the physical adsorption. All that allows us to conclude that the proposed nonlinear mechanism of generating the repulsive part of the adsorption potential can be relevant in realistic setups. In contrast to other mechanisms considered, e.g., in Refs. [48–50], which rely on special geometries or special tuning of the material constants, the proposed nonlinear mechanism is *generic*. Nanosize objects are usually characterized by sizable values of nonlinear polarizability [83], so one may expect that this mechanism will always be responsible for a substantial part of the repulsive interaction. The present theory becomes inapplicable only in the case of weak nonlinearity, when the contribution of nonlinear effects provides a repulsive core at distances smaller than the

particle radius, so that one has to take into account chemical interactions.

As mentioned above, the properties of the repulsive part of the Casimir-Lifshitz potential are under active discussion in the literature (see Refs. [43–51]). Particularly, in Ref. [47] the existence of repulsive Casimir-Lifshitz forces acting at relatively large distances (about 10 nm) has been demonstrated experimentally. Although the existence of long-range repulsive forces is in line with our theoretical proposal, we cannot make a direct comparison of those experimental results with our theory, because the experiment has been performed on large objects (spheres of 38.9 μm radius), while our theoretical approach is only applicable to nanosized particles since we make use of the near-field approximation.

At the same time, it should be noted that our approach neglects the influence of higher multipole moments, which is often necessary for nonpointlike particles [84–87]. In order to account for the contribution of multipole moments into the Casimir-Lifshitz potential, one can either include the higher multipoles into the theory simultaneously with the nonlinear polarizability, or reformulate the theory in terms of induced local currents; the detailed treatment of this problem is beyond the scope of the present work. Our main goal here was to show that the presence of nonlinear polarizability may lead to the formation of the repulsive part of the adsorption potential even in the absence of the contributions from higher multipoles.

In order to compare our findings with the known results of theoretical studies [84–87] of repulsive dispersion forces, in Fig. 7 we present the normalized interaction potential in the so-called PFA (proximity-force approximation) units. For instance, in Ref. [85] a repulsive dispersion interaction has been obtained as a result of taking into account multipole moments. Comparing our results for the repulsive interaction caused by nonlinearity to those of Ref. [85] (see the curve labeled "small-sphere limit" in the inset of Fig. 7), one can see that irrespective of the specific nature of the repulsive
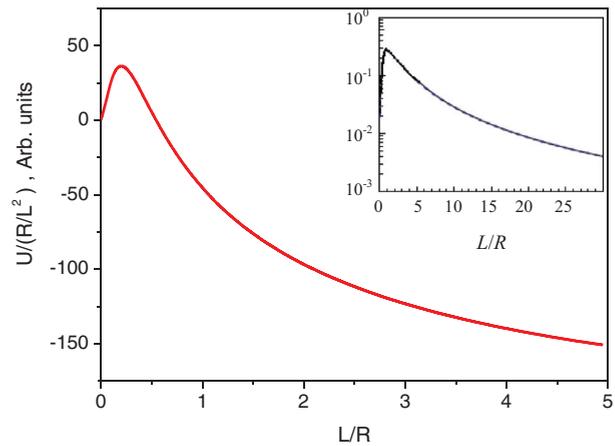
FIG. 7. (Color online) The normalized interaction potential $\rho = U(d)/(R/L^2)$ in terms of a ratio to the PFA [85], where R is the particle radius and L is the distance between the adsorbent surface and the particle surface, for a spherical particle of the radius $R_p = 10$ nm with $\varepsilon_p = 11.8$ at the adsorbent with $\varepsilon_s = 3$. The inset shows the results of Ref. [85].

interaction, the qualitative behavior of the $U(d)/(R/L^2)$ curve remains the same. At the quantitative level, the effects of nonlinearity yield larger contribution at small distances. This comparison emphasizes once again that the method developed here is valid for nanosized particles.

In the limit of a pointlike object, the interaction potential transforms into the potential describing the interaction of a molecule with a solid surface by means of the mode softening mechanism considered in Refs. [31,32]. Since a nanoparticle is characterized by a broad excitation spectrum, such a mechanism of the adsorption potential formation might be valid for nanoparticles as well.

When the nonlinear porarizability is neglected ($\beta \to 0$), the adsorption potential transforms to the van der Waals adsorption potential for a nonpoint particle, which, in turn, becomes the usual $-1/d^6$ potential of the van der Waals interaction in the case of a pointlike particle [72].

We have also applied our approach to study the particle-surface interaction in the presence of the surface plasmon polariton propagating along the interface, and have shown that the excitation of the surface wave leads to a sharp increase of the binding energy.

The developed approach can be useful for the study of the interaction between biological nanosized objects (e.g., viruses) and nanostructured surfaces. Our studies corroborate the ideas discussed in Ref. [25], namely that interaction with a nanostructured surface bearing an excited surface plasmon polariton can lead to selective adsorption of nano-objects, which, particularly, can serve as a base for developing innovative antiviral therapy methods.

[1] S. R. Morrison, *The Chemical Physics of Surfaces* (Plenum Press, New York, 1977).

[2] S.-H. Park, J.-H. Im, J.-W. Im, B.-H. Chun, and J.-H. Kim, Microchem. J. **63**, 71 (1999).

[3] *Surface-Enhanced Raman Scattering, Physics and Applications*, Topics in Applied Physics Vol. 103, edited by K. Kneipp, M. Moskovits, and H. Kneipp (Springer, Berlin, 2006).

[4] Y. S. Huh, A. J. Chung, and D. Erickson, Microfluid. Nanofluid. **6**, 285 (2009).

[5] J. S. Biteen, L. A. Sweatlock, H. Mertens, N. S. Lewis, A. Polman, and H. A. Atwater, J. Phys. Chem. C **111**, 13372 (2007).

[6] P. Mandal, P. Gupta, A. Nandi, and S. A. Ramakrishna, J. Nanophoton. **6**, 063527 (2012).

[7] S. Chandra, J. Doran, S. J. McCormack, M. Kennedy, and A. J. Chatten, Sol. Energy Mater. Sol. Cells **98**, 385 (2012).

[8] T. Kurihara, R. Sugimoto, R. Kudo, S. Takahashi, and K. Takamasu, Int. J. Nanomanuf. **8**, 419 (2012).

[9] Y. Engel, J. D. Schiffman, J. M. Goddard, and V. M. Rotello, Mater. Today **15**, 478 (2012).

[10] A. P. Malshe, K. P. Rajurkar, K. R. Virwani, C. R. Taylor, D. L. Bourell, G. Levy, M. M. Sundaram, J. A. McGeough, V. Kalyanasundaram, and A. N. Samant, CIRP Ann. **59**, 628 (2010).

[11] P. K. Hansma, V. B. Elings, O. Marti, and C. E. Bracker, Science **242**, 209 (1988).

[12] N. J. Tao, Phys. Rev. Lett. **76**, 4066 (1996).

[13] H. Heinzelmann and D. W. Pohl, Appl. Phys. A **59**, 89 (1994).

[14] A. Zybin, Y. A. Kuritsyn, E. L. Gurevich, V. V. Temchura, K. Überla, and K. Niemax, Plasmonics **5**, 31 (2010).

[15] S. Wang, X. Shan, U. Patel, X. Huang, J. Lu, J. Li, and N. Tao, Proc. Natl. Acad. Sci. USA **107**, 16028 (2010).

[16] V. Lozovski, J. Comput. Theor. Nanosci. **9**, 859 (2012).

[17] R. Ciriminna, P. D. Carà, M. Sciortino, and M. Pagliaro, Adv. Synth. Catal. **353**, 677 (2011).

[18] K. Philippot and P. Serp, in *Nanomaterials in Catalysis*, 1st ed., edited by P. Serp and K. Philippot (Wiley, Weinheim, 2013), p. 1–54.

[19] V. Hlady and J. Buijs, Curr. Opin. Biotechnol. **7**, 72 (1996).

[20] I. Fenoglio, Adv. Drug Delivery Rev. **63**, 1186 (2011).

[21] M. S. A. Baksh and R. T. Yang, AIChE J. **38**, 1357 (1992).

[22] L. Zhang, F. X. Gu, J. M. Chan, A. Z. Wang, R. S. Langer, and O. C. Farokhzad, Clin. Pharmacol. Ther. **83**, 761 (2008).

[23] W.-T. Liu, J. Biosci. Bioeng. **102**, 1 (2006)

[24] V. Lozovski, V. Lysenko, V. Piatnytsia, O. Scherbakov, N. Zholobak, and M. Spivak, J. Bionanosci. **6**, 109 (2012).

[25] V. Lysenko, V. Lozovski, M. Spivak, Ukr. J Phys. **58**, 77 (2013).

[26] J. Mahanty and B. W. Ninham, *Dispersion Forces* (Academic, New York, 1976).

[27] S. Das'Sarma and S.-M. Paik, Chem. Phys. Lett. **126**, 526 (1986).

[28] N. S. Maurya, A. K. Mittal, and P. Cornel, J. Environ. Biol. **29**, 31 (2008).

[29] M. R. Rosene, M. Ozcan, and M. Manes, J. Phys. Chem. **80**, 2586 (1976).

[30] D. F. Klemperer and J. C. Snaith, J. Vac. Sci. Technol. **9**, 925 (1972).

[31] L. W. Bruch and Th. W. Ruijgrok, Surf. Sci. **79**, 509 (1979).

[32] G. Vidali, M. W. Cole, and J. R. Klein, Phys. Rev. B **28**, 3064 (1983).

[33] F. G. Bass and V. Z. Lozovski, Phys. Rev. B **58**, 10721 (1998).

[34] I. Baraille, M. Rerat, and P. Mora, Phys. Rev. B **73**, 075410 (2006).

[35] B. I. Khudik and V. Z. Lozovski, Phys. Status Solidi B **158**, 511 (1990).

[36] B. I. Khudik and V. Z. Lozovski, Phys. Status Solidi B **160**, 137 (1990).

[37] H. B. G. Casimir, Proc. K. Ned. Akad. Wet. **51**, 793 (1948).

[38] H. B. G. Casimir and D. Polder, Phys. Rev. **73**, 360 (1948).

[39] E. M. Lifshitz, Dokl. Akad. Nauk. SSSR **97**, 643 (1954).

[40] E. M. Lifshitz, Dokl. Akad. Nauk. SSSR **100**, 879 (1955).

[41] E. M. Lifshitz, Sov. Phys. JETP **29**, 94 (1955).

[42] I. E. Dzyaloshinskii, E. M. Lifshitz, and L. P. Pitaevskii, Sov. Phys. JETP **37**, 229 (1959); see also I. E. Dzyaloshinskii, E. M. Lifshitz, and L. P. Pitaevskii, Sov. Phys. Usp. **4**, 153 (1961).

[43] C. J. Van Oss, D. R. Absolom, and A. W. Neumann, Colloids Surf. **1**, 45 (1980).

[44] E. Buks and M. L. Roukes, Nature **419**, 119 (2002).

[45] O. Kenneth, I. Klich, A. Mann, and M. Revzen, Phys. Rev. Lett. **89**, 033001 (2002).

[46] O. Kenneth and I. Klich, Phys. Rev. Lett. **97**, 160401 (2006).

[47] J. N. Munday, F. Capasso, and V. A. Parsegian, Nature **457**, 170 (2009).

[48] L. P. Pitaevskii, presented at New Frontiers in Casimir Force Control, Santa Fe, NM, 27–29 September 2009, available at http://cnls.lanl.gov/casimir/PresentationsSF/Repulsive_force09.pdf.

[49] M. Levin, A. P. McCauley, A. W. Rodriguez, M. T. Homer Reid, and S. G. Johnson, Phys. Rev. Lett. **105**, 090403 (2010).

[50] K. A. Milton, E. K. Abalo, P. Parashar, N. Pourtolami, I. Brevik, and S. Å. Ellingsen, Phys. Rev. A **83**, 062507 (2011); see also arXiv:1202.6415v2 [hep-th] (2012).

[51] M. Boström and B. E. Sernelius, Phys. Rev. A **85**, 012508 (2012).

[52] G. Y. Panasyuk, J. C. Schotland, and V. A. Markel, Phys. Rev. Lett. **100**, 047402 (2008).

[53] A. A. Govyadinov, G. Y. Panasyuk, J. C. Schotland, and V. A. Markel, Phys. Rev. B **84**, 155461 (2011).

[54] D. Kandpal, S. Kalele, and S. K. Kulkarni, Pramana **69**, 277 (2007).

[55] T. Klar, M. Perner, S. Grosse, G. von Plessen, W. Spirkl, and J. Feldmann, Phys. Rev. Lett. **80**, 4249 (1998).

[56] M. Nikbakht and M. H. Mahdieh, J. Eur. Opt. Soc.: Rapid Publ. **7**, 12025 (2012).

[57] A. Grubisic, E. Ringe, C. M. Cobley, Y. Xia, L. D. Marks, R. P. Van Duyne, and D. J. Nesbitt, Nano Lett. **12**, 4823 (2012).

[58] T. Nakamura, N. Hirata, Y. Sekino, S. Nagaoka, and A. Nakajima, J. Phys. Chem. C **114**, 16270 (2010).

[59] O. Keller, Phys. Rep. **268**, 85 (1996).

[60] C. Girard, C. Joachim, and S. Gauthier, Rep. Prog. Phys. **63**, 893 (2000).

[61] A. V. Goncharenko, Phys. Rev. E **68**, 041108 (2003).

[62] H. Chen, X. Kou, Z. Yang, W. Ni, and J. Wang, Langmuir **24**, 5233 (2008).

[63] A. Albanese, P. S. Tang, and W. C. W. Chan, Annu. Rev. Biomed. Eng. **14**, 1 (2012).

[64] P. K. Jain, K. S. Lee, I. H. El-Sayed, and M. A. El-Sayed, J. Phys. Chem. B **110**, 7238 (2006).

[65] V. Lozovski, J. Comput. Theor. Nanosci. **7**, 2077 (2010).

[66] P. L. Silvestrelli and A. Ambrosetti, Phys. Rev. B **87**, 075401 (2013).

[67] E. V. Chenskii and V. V. Tarasenko, Sov. Phys. JETP **56**, 618 (1982).

[68] D. R. S. Talbot and J. R. Willis, IMA J. Appl. Math. **35**, 39 (1985).

[69] L. Yang and K. Dayal, J. Comput. Phys. **230**, 7821 (2011).

[70] V. Lozovski, Yu. Nazarok, and S. I. Bozhevolnyi, Physica E **11**, 323 (2001).

[71] O. Keller, M. Xiao, and S. Bozhevolnyi, Surf. Sci. **280**, 217 (1993).

[72] Yu. S. Barash and V. L. Ginzburg, Sov. Phys. Usp. **27**, 467 (1984).

[73] Yu. S. Barash, *Van der Waals Forces* (Nauka, Moscow, 1988) [in Russian]; Yu. S. Barash and V. L. Ginzburg, Sov. Phys. Usp. **18**, 305 (1975).

[74] V. L. Ginzburg, Radiophys. Quantum Electron. [Engl. Transl.] **28**, 839 (1985).

[75] M. Mansuripur and D. P. Tsai, Opt. Commun. **284**, 707 (2011).

[76] R. J. Potton, Rep. Prog. Phys. **67**, 717 (2004).

[77] G. C. Wick, Phys. Rev. **80**, 268 (1950).

[78] T. S. Evans and D. A. Steer, Nucl. Phys. B **474**, 481 (1996).

[79] R. W. Boyd and G. L. Fischer, in *Encyclopedia of Materials: Science and Technology*, 2nd ed. (Elsevier, Amsterdam, 2001), pp. 6237–6244.

[80] S.-w. Lee and W. M. Sigmund, Colloids Surf. A **204**, 43 (2002).

[81] O. Keller and P. Sønderkær, Proc. SPIE **954**, 344 (1988).

[82] A. A. Maradudin, in *Surface Polaritons*, edited by W. M. Agranovich and D. L. Mills (North-Holland, Amsterdam, 1982).

[83] R. W. Boyd, *Nonlinear Optics*, 2nd ed. (Academic Press, San Diego, CA, 2003).

[84] C. Girard and C. Girardet, J. Chem. Phys. **86**, 6531 (1987).

[85] P. A. Maia Neto, A. Lambrecht, and S. Reynaud, Phys. Rev. A **78**, 012115 (2008).

[86] A. Canaguier-Durand, P. A. Maia Neto, I. Cavero-Pelaez, A. Lambrecht, and S. Reynaud, Phys. Rev. Lett. **102**, 230404 (2009).

[87] A. Canaguier-Durand, A. Gerardin, R. Guerout, P. A. Maia Nato, V. V. Nesvizhevsky, A. Yu. Voronin, A. Lambrecht, and S. Reynaud, Phys. Rev. A **83**, 032508 (2011).